Ancient helium and tungsten isotopic signatures preserved in mantle domains least modified by crustal recycling

Matthew G. Jackson[a,1] , Janne Blichert-Toft[b,2] , Saemundur A. Halldórsson[c,2] , Andrea Mundl-Petermeier[d] , Michael Bizimis[e] , Mark D. Kurz[f], Allison A. Price[a], Sunna Harðardóttir[c], Lori N. Willhite[a,g] , Kresten Breddam[h], Thorsten W. Becker[i,j] , and Rebecca A. Fischer[k]

[a]Department of Earth Science, University of California, Santa Barbara, CA 93106-9630; [b]Laboratoire de Géologie de Lyon, Ecole Normale Supérieure de Lyon, CNRS, and Université de Lyon, 69007 Lyon, France; [c]NordVulk, Institute of Earth Sciences, University of Iceland, 102 Reykjavík, Iceland; [d]Department of Lithospheric Research, University of Vienna, 1090 Vienna, Austria; [e]School of the Earth, Ocean and Environment, University of South Carolina, Columbia, SC 29208; [f]Department of Marine Chemistry, Woods Hole Oceanographic Institution, Woods Hole, MA 02543; [g]Department of Geology, University of Maryland, College Park, MD 20742; [h]Radiation Protection, Danish Health Authority, 2300 Copenhagen, Denmark; [i]Institute for Geophysics, The Jackson School of Geosciences, The University of Texas at Austin, Austin, TX 78713; [j]Department of Geological Sciences, The Jackson School of Geosciences, The University of Texas at Austin, Austin, TX 78713; and [k]Department of Earth & Planetary Sciences, Harvard University, Cambridge, MA 02138

Rare high-^{3}He/^{4}He signatures in ocean island basalts (OIB) erupted at volcanic hotspots derive from deep-seated domains preserved in Earth's interior. Only high-^{3}He/^{4}He OIB exhibit anomalous ^{182}W—an isotopic signature inherited during the earliest history of Earth—supporting an ancient origin of high ^{3}He/^{4}He. However, it is not understood why some OIB host anomalous ^{182}W while others do not. We provide geochemical data for the highest-^{3}He/^{4}He lavas from Iceland (up to 42.9 times atmospheric) with anomalous ^{182}W and examine how Sr-Nd-Hf-Pb isotopic variations—useful for tracing subducted, recycled crust—relate to high ^{3}He/^{4}He and anomalous ^{182}W. These data, together with data on global OIB, show that the highest-^{3}He/^{4}He and the largest-magnitude ^{182}W anomalies are found only in geochemically depleted mantle domains—with high ^{143}Nd/^{144}Nd and low ^{206}Pb/^{204}Pb—lacking strong signatures of recycled materials. In contrast, OIB with the strongest signatures associated with recycled materials have low ^{3}He/^{4}He and lack anomalous ^{182}W. These observations provide important clues regarding the survival of the ancient He and W signatures in Earth's mantle. We show that high-^{3}He/^{4}He mantle domains with anomalous ^{182}W have low W and ^{4}He concentrations compared to recycled materials and are therefore highly susceptible to being overprinted with low ^{3}He/^{4}He and normal (not anomalous) ^{182}W characteristic of subducted crust. Thus, high ^{3}He/^{4}He and anomalous ^{182}W are preserved exclusively in mantle domains least modified by recycled crust. This model places the long-term preservation of ancient high ^{3}He/^{4}He and anomalous ^{182}W in the geodynamic context of crustal subduction and recycling and informs on survival of other early-formed heterogeneities in Earth's interior.

mantle geochemistry | hotspot volcanism | ^{182}W | ^{3}He/^{4}He | Hadean

Plate tectonic motions deliver oceanic and continental crust into the mantle at subduction zones. Following residence times of ~2 Ga, subducted crustal material is returned to the shallow mantle in buoyantly upwelling conduits of hot mantle material, known as mantle plumes, where they are partially melted and erupted as ocean island basalts (OIB) at volcanic hotspots (1–3). Recycled materials contribute to a variety of geochemically distinct mantle components often referred to as EM1 (enriched mantle I), EM2 (enriched mantle II), and HIMU (high "μ" or high ^{238}U/^{204}Pb) (1–3). While there is debate surrounding the exact nature of the recycled protoliths responsible for these mantle endmembers (4–7), they are likely generated by input of shallow geochemical reservoirs into the deep Earth. The three mantle components have ^{87}Sr/^{86}Sr, ^{143}Nd/^{144}Nd, ^{176}Hf/^{177}Hf, and ^{206}Pb/^{204}Pb distinct from the depleted mantle (DM) sampled by basalts erupted at midocean ridges (MORB). In three-dimensional (3D)

Sr-Nd-Pb isotopic space, these four geochemical endmembers can be used to define the apices of a tetrahedron (8) (Fig. 1) and have low ^{3}He/^{4}He, similar to, or lower than, MORB (8 ± 2 Ra, ratio to atmosphere) (9). An additional mantle component is found internal to the other four and, like DM, is characterized by geochemically depleted compositions that relate to long-term crustal extraction from the mantle, which changes the parent–daughter ratios that govern key radiogenic isotopic systems, resulting in high ^{143}Nd/^{144}Nd and ^{176}Hf/^{177}Hf coupled with low ^{87}Sr/^{86}Sr and ^{206}Pb/^{204}Pb. Existing long-lived radiogenic isotopic data show that this fifth component is geochemically depleted (8, 10) and has been variously referred to as FOZO [focus zone (8)], PHEM [primordial helium mantle (11)], or C [common (12)]. In contrast to DM, this geochemically depleted mantle composition was argued to exhibit elevated ^{3}He/^{4}He (8), signaling the preservation of an ancient reservoir in the deep Earth (13).

Significance

The recent discovery of anomalous ^{182}W signatures in modern, plume-derived hotspot lavas provides evidence for survival of domains in Earth's interior since the early Hadean. Only lavas with ancient, high-^{3}He/^{4}He signatures preserve anomalous ^{182}W signatures. However, it is not known why only high-^{3}He/^{4}He lavas have anomalous ^{182}W, while other hotspot lavas do not. We show that only hotspot lavas lacking strong recycled crust signatures exhibit high ^{3}He/^{4}He and anomalous ^{182}W. This observation is explained by subduction of W- and ^{4}He-rich crust that has low ^{3}He/^{4}He and normal ^{182}W: Following subduction, the crust masks high-^{3}He/^{4}He and anomalous ^{182}W signatures characteristic of ancient mantle domains. Our model links destruction of Hadean geochemical signatures with the geodynamic process of plate subduction and recycling.

Fig. 1. Mantle tetrahedron showing that most of the highest $^3He/^4He$ lavas in Iceland, and global hotspots, do not overlap with the common mantle component [shown as ellipsoid (27)]. Four different high-$^3He/^4He$ (>25 Ra) components in Iceland (Vestfirðir, ERZ, SIVZ, and Baffin Island) are shown. The highest $^3He/^4He$ (>30 Ra) samples from each global oceanic hotspot with available Sr-Nd-Pb isotopes—Galapagos, Hawaii, and Samoa—are also shown (data sources for these additional lavas are in *SI Appendix*, Fig. S4). EM1, EM2, and HIMU apices of the tetrahedron are published elsewhere (27), as is MORB (63), but EM2 extends to more extreme compositions (36) (indicated by arrow). Data for the highest $^3He/^4He$ lavas with available Sr-Nd-Pb isotopes from the different Iceland high-$^3He/^4He$ (>25 Ra) localities are from Dataset S1; the Baffin Island lava is the highest $^3He/^4He$ (39.9 Ra) lava that is the least crustally contaminated (23). Measured values are shown for all lavas except for Baffin Island, where both age-corrected (c) and measured compositions are shown: The calculated present-day Baffin Island mantle source is indistinguishable from the measured composition in the figure [see (23) and *SI Appendix*, Fig. S4 legend for details of the age correction and present-day source calculation].

Recent discoveries employing the short-lived ^{182}Hf-^{182}W isotopic systematics have demonstrated the presence of anomalous, negative $\mu^{182}W$ (where μ is the deviation of $^{182}W/^{184}W$ from the terrestrial standard in parts per million) in modern OIB (14–17), and the anomalies are found uniquely in lavas with high $^3He/^4He$ (14–16). ^{182}W anomalies were generated only while the parent nuclide ($^{182}Hf \rightarrow {}^{182}W + 2\beta^-$, half-life = 8.9 million years) was extant (i.e., <60 Ma following Solar System formation), so the observation of anomalous ^{182}W signals in the modern mantle implies that these signatures have been preserved in Earth since the early Hadean. This is consistent with the discovery of heterogeneous ^{129}Xe and ^{142}Nd—which are products of the short-lived isotopes ^{129}I and ^{146}Sm, respectively, extant only in the Hadean (18, 19)—in the modern mantle, further supporting the observation of chemical heterogeneities preserved in Earth's interior since the Hadean.

An important recent observation is that ^{182}W and $^3He/^4He$ data from oceanic basalts define a negatively sloping array, with anomalous ^{182}W signatures in OIB uniquely associated with lavas that exhibit high $^3He/^4He$ (14–16). This fundamental advance relates primordial high $^3He/^4He$ with an early-formed isotopic heterogeneity. However, several outstanding questions regarding ^{182}W systematics in the modern mantle remain: 1) What is the mechanism responsible for the unique association of anomalous $\mu^{182}W$ with high-$^3He/^4He$ hotspot lavas, and why do low-$^3He/^4He$ lavas lack ^{182}W anomalies? 2) Do the geodynamic processes of subduction and recycling impact the ^{182}W-$^3He/^4He$ mantle array? 3) Do ^{182}W systematics exhibit relationships with isotopic tracers (i.e., Sr-Nd-Pb) sensitive to crustal subduction and recycling, or

are ^{182}W systematics somehow insensitive to these geodynamic processes such that Sr-Nd-Pb isotope systematics are decoupled from ^{182}W?
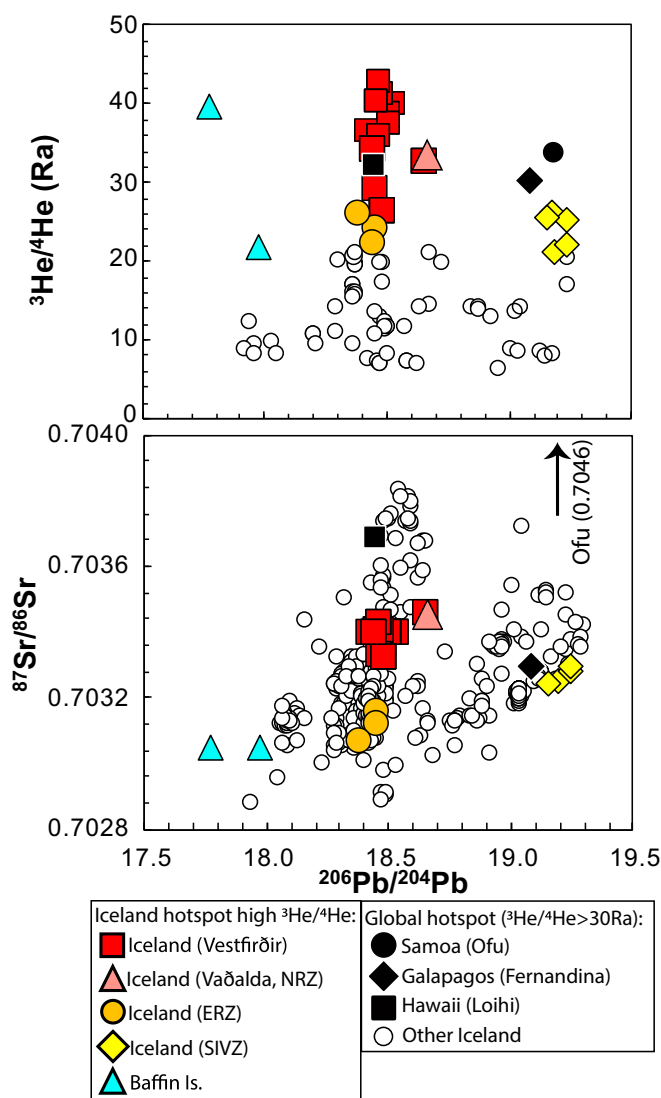
In order to address these outstanding questions, we provide a large geochemical dataset on high-$^3He/^4He$ lavas from the Iceland hotspot and examine the data in the context of new global OIB datasets combining He, Sr, Nd, Hf, and Pb isotopes with W isotopes. The data and analysis provide insights into the mechanisms for preservation of anomalous ^{182}W and high-$^3He/^4He$ signatures in the mantle.

Results

We present He-Sr-Nd-Hf-Pb-W isotopic data (*Materials and Methods*) on a suite of 28 basalt samples from all Icelandic localities known to have high $^3He/^4He$ (>25 Ra): mid-Miocene lavas from northwest Iceland (Vestfirðir) as well as Neovolcanic zone lavas from the Eastern Rift Zone (ERZ), the South Iceland Volcanic Zone (SIVZ), and Vaðalda shield volcano in the Northern Rift Zone (NRZ) (20–22) (*SI Appendix*, Fig. S1 and Datasets S1, S2, and S3). These data are presented together with published data (23) from ~60 Ma Baffin Island and West Greenland (BIWG) flood basalt lavas, an additional high-$^3He/^4He$ [up to 50 Ra (23–26)] locality on the Iceland hotspot track. Helium, Pb, and W isotopic data on a small subset (n = 8, 9, and 10, respectively) of the Iceland samples examined here (14, 15), as well as $^3He/^4He$ data on a different subset of 10 samples (20, 22), were published previously. The dataset presented here includes $^{87}Sr/^{86}Sr$ and $^{143}Nd/^{144}Nd$ for all 28 samples and $^{176}Hf/^{177}Hf$ and Pb isotopic measurements for 27 and 19 samples, respectively. We also present $^3He/^4He$ measurements by coupled vacuum crushing and fusion of olivine and clinopyroxene crystals on 10 samples (including one sample with the highest $^3He/^4He$ in the dataset, 42.9 Ra; Fig. 2 and *SI Appendix*, Fig. S2) and $^3He/^4He$ measurements by fusion on the same powders from nine samples with previously published $^3He/^4He$ by crushing (15). We present a W isotopic measurement on the highest $^3He/^4He$ ERZ lava, complementing 10 prior measurements made on this suite of 28 samples (15) [additional ^{182}W analyses on a different suite of six Icelandic lavas are also available (15)]. Additionally, we present major and trace element data for all of the mid-Miocene Vestfirðir lavas and a subset of the Neovolcanic zone lavas (*SI Appendix*, Fig. S3). Our data and published data on the 28 samples of this study represent a full geochemical characterization of all known high-$^3He/^4He$ localities in Iceland.

Our Iceland dataset, combined with Sr-Nd-Pb isotope data from the literature, expands the number of OIB samples characterized for both ^{182}W (14–17) and Sr-Nd-Pb isotopic compositions by nearly 60% (Dataset S4). This augmented dataset allows examination of relationships between Sr-Nd-Pb isotopes, traditionally used to detect signatures of crustal recycling, and $^3He/^4He$ and ^{182}W, which can trace early-formed reservoirs in Earth.

In Fig. 2 and *SI Appendix*, Fig. S4, the He-Sr-Nd-Hf-Pb isotopic compositions for most (~75%) of the Iceland lavas with $^3He/^4He$ >21 Ra are presented and show that the highest $^3He/^4He$ lavas sample four high-$^3He/^4He$ components with distinct Sr-Nd-Hf-Pb isotopic compositions. The Vestfirðir (up to 42.9 Ra) and Vaðalda (33.6 Ra) lavas are similar geochemically and are grouped together. The Vaðalda lava shows the recent (Pleistocene) reappearance of a geochemical component not known in Iceland since the mid-Miocene (Fig. 2 and *SI Appendix*, Fig. S4). The ERZ lavas host a second Iceland high-$^3He/^4He$ component (25.9 Ra; Dataset S1) with Sr-Nd-Hf isotopic ratios more geochemically depleted than Vestfirðir and Vaðalda lavas. The SIVZ lavas represent a third Iceland high-$^3He/^4He$ component [25.7 to 26.2 Ra (20); Dataset S1] with $^{206}Pb/^{204}Pb$ higher than the other two components. A fourth high-$^3He/^4He$ Iceland component is evident in previously published geochemical datasets from BIWG,

Fig. 2. Relationships between $^3He/^4He$, $^{87}Sr/^{86}Sr$, and $^{206}Pb/^{204}Pb$ in Iceland hotspot lavas showing four geochemically distinct high-$^3He/^4He$ Iceland components (Vestfirðir, ERZ, SIVZ, and Baffin Island). The highest $^3He/^4He$ lavas from Hawaii, Galapagos, and Samoa also exhibit heterogeneous Sr-Nd-Pb isotopic compositions. Data sources for these lavas are in *SI Appendix*, Fig. S4. Only the least crustally contaminated Baffin Island lavas are shown (23). Measured heavy radiogenic isotopic compositions are shown for all samples except for Baffin Island, where present-day mantle source values are plotted (23) [see (23) and *SI Appendix*, Fig. S4 legend for details of present-day source calculation]. For Iceland hotspot lavas, only high-precision Pb isotopic data (MC-ICP-MS and double-spike TIMS) are shown. (*Top*) The colored symbols represent lavas with $^3He/^4He$ >21 Ra sampling all known high-$^3He/^4He$ regions of the Iceland hotspot—ERZ, SIVZ, NRZ (Vaðalda), Vestfirðir, and BIWG—and white symbols represent Iceland lavas (all of which have $^3He/^4He$ <21 Ra) from the other regions of Iceland. (*Bottom*) Colored symbols represent lavas with $^3He/^4He$ >21 Ra sampling all known high-$^3He/^4He$ regions of the Iceland hotspot, and the white symbols represent Iceland lavas with $^3He/^4He$ ≤21 Ra (or lavas that have not been characterized for $^3He/^4He$).

which have $^3He/^4He$ up to 50 Ra, the highest known terrestrial mantle-derived $^3He/^4He$ (23–26); after applying major and trace element filters for continental crust assimilation (23), the Baffin Island lavas exhibit the lowest $^{206}Pb/^{204}Pb$ identified along the Iceland hotspot track (Fig. 2).

The four geochemically distinct high-$^3He/^4He$ Iceland components are clearly resolved in Sr-Nd-Hf-Pb isotope space (Fig. 2

and *SI Appendix*, Fig. S4), and the range in $^{206}Pb/^{204}Pb$ across the four Iceland high-$^3He/^4He$ components found at five geographic locations—Vestfirðir/Vaðalda, ERZ, SIVZ, and BIWG—spans a remarkable ∼40% of the total variability found in global OIB (Fig. 2 and *SI Appendix*, Fig. S4). The wide range of Sr-Nd-Hf-Pb isotopic compositions in Icelandic and global (including Hawaii, Samoa, and Galapagos) high-$^3He/^4He$ (>25 Ra) lavas is notable. Nonetheless, high-$^3He/^4He$ lavas globally exhibit geochemically depleted Sr-Nd-Hf isotopic signatures and relatively unradiogenic $^{206}Pb/^{204}Pb$ compositions ($^{206}Pb/^{204}Pb$ <19.5) (Fig. 2 and *SI Appendix*, Fig. S4), where the chondritic reference frame for $^{143}Nd/^{144}Nd$ and $^{176}Hf/^{177}Hf$ serves as a reference point for geochemical depletion: Geochemically depleted lavas have $^{143}Nd/^{144}Nd$ and $^{176}Hf/^{177}Hf$ ratios higher than chondrites (i.e., as shown for $^{143}Nd/^{144}Nd$ in Fig. 3). Complementing negative $\mu^{182}W$ anomalies observed in high-$^3He/^4He$ hotspot lavas globally (14–16), Vestfirðir and SIVZ lavas have negative $\mu^{182}W$ anomalies (15), and we further report here another resolvable negative $\mu^{182}W$ anomaly (-10.0 ± 3.8) in the highest $^3He/^4He$ ERZ lava (Dataset S2). However, recently published ^{182}W measurements of the high-$^3He/^4He$ BIWG lavas do not reveal $\mu^{182}W$ anomalies (15), which is discussed below.
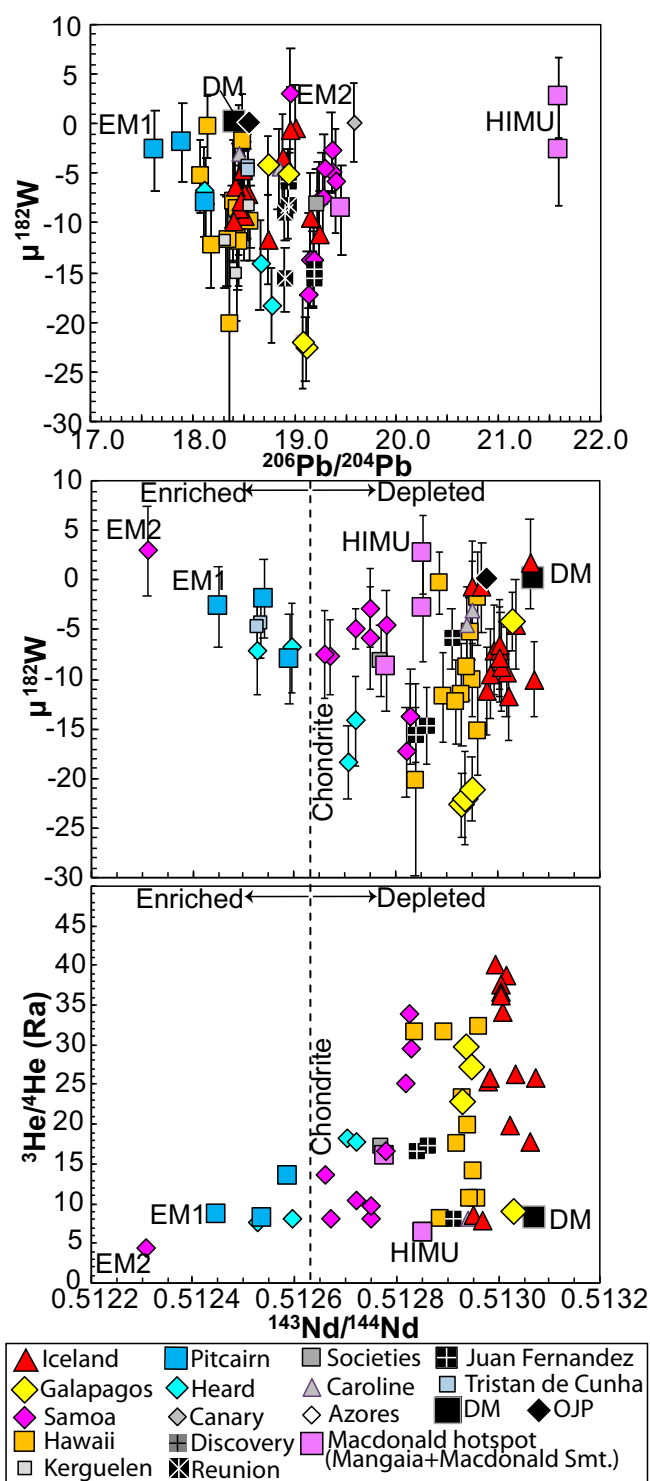
In Fig. 1, Sr-Nd-Pb isotopic compositions of the lavas that define the four Iceland high-$^3He/^4He$ components, and the highest $^3He/^4He$ lavas from other hotspots, are compared with the common mantle component. This component is shown as an ellipsoid and represents the 95% confidence interval for the volume encompassing the best-fit intersections of the trendlines that were fit to OIB arrays formed by individual hotspots (27), as this component (i.e., FOZO) was originally defined by the intersection of global OIB arrays (8) (but we note that not all OIB arrays extend into the common component region). In Iceland, only the highest $^3He/^4He$ lava from the SIVZ plots within the common mantle component ellipsoid, while the highest $^3He/^4He$ ERZ, Vestfirðir, and Baffin Island lavas are shifted toward compositions more geochemically depleted (and in the case of Baffin Island, more similar to MORB) than the common mantle component. Among the other hotspots globally with $^3He/^4He$ >25 Ra, only the Galapagos high-$^3He/^4He$ lava (30.3 Ra) plots within the ellipsoid, while Hawaiian (32.3 Ra) and Samoan (33.4 Ra) high-$^3He/^4He$ lavas do not (Fig. 1). In summary, most of the highest $^3He/^4He$ OIB globally are not necessarily associated with the common mantle component in Sr-Nd-Pb isotopic space, as previously defined. Due to this isotopic variability, we do not refer to the high-$^3He/^4He$ mantle domain with anomalous ^{182}W as FOZO, C, or PHEM, all of which share geochemically depleted characteristics.

The geochemically depleted high-$^3He/^4He$ mantle is most clearly distinguished from the geochemically depleted DM by having high $^3He/^4He$ and anomalous ^{182}W. However, due to extreme geochemical depletion in some high-$^3He/^4He$ lavas (in particular the BIWG lavas), we are not able to specify which mantle domain, DM or high-$^3He/^4He$, extends to more geochemically depleted compositions. Nonetheless, we show that only geochemically depleted mantle domains have the largest magnitude $\mu^{182}W$ anomalies. The exclusive association of the largest magnitude $\mu^{182}W$ anomalies with geochemically depleted mantle (i.e., superchondritic $^{143}Nd/^{144}Nd$ and $^{176}Hf/^{177}Hf$) provides key insights into processes responsible for the preservation, and destruction, of ^{182}W anomalies in Earth's interior.

Discussion

Influence of Recycled Crust on High-$^3He/^4He$ and Anomalous ^{182}W Signatures in the Mantle. An important issue in chemical geodynamics is how short-lived radiogenic isotopic signatures generated in the Hadean Earth—^{182}W, ^{142}Nd, and ^{129}Xe—have survived in the convecting mantle to be sampled by modern OIB (16–19). The presence of high $^3He/^4He$ and anomalous ^{182}W in

Fig. 3. Relationships between $^3He/^4He$, $\mu^{182}W$, $^{143}Nd/^{144}Nd$, and $^{206}Pb/^{204}Pb$ in global OIB showing that only geochemically depleted OIB (i.e., high $^{143}Nd/^{144}Nd$ and low $^{206}Pb/^{204}Pb$) lacking recycled crust signatures host the highest $^3He/^4He$ and largest-magnitude $\mu^{182}W$ anomalies. The compilation of He-Sr-Nd-Pb isotopes (from this study and prior studies; Dataset S4) for lavas with available $\mu^{182}W$ shows that only lavas with low $^{206}Pb/^{204}Pb$ (*Top*) or high $^{143}Nd/^{144}Nd$ (*Middle*) host the most extreme negative $\mu^{182}W$ anomalies. Lavas with the most extreme negative $\mu^{182}W$ anomalies also exhibit high $^3He/^4He$ (*Bottom*, where only lavas with available $\mu^{182}W$ data are shown). In contrast, the mantle endmembers EM1, EM2, and HIMU have low $^3He/^4He$ and lack anomalous $\mu^{182}W$, as does DM. The chondritic reference $^{143}Nd/^{144}Nd$ is published elsewhere (64). All data and error bars (2σ) are provided in Dataset S4. The $^{143}Nd/^{144}Nd$ and $^{206}Pb/^{204}Pb$ for OJP is an average of
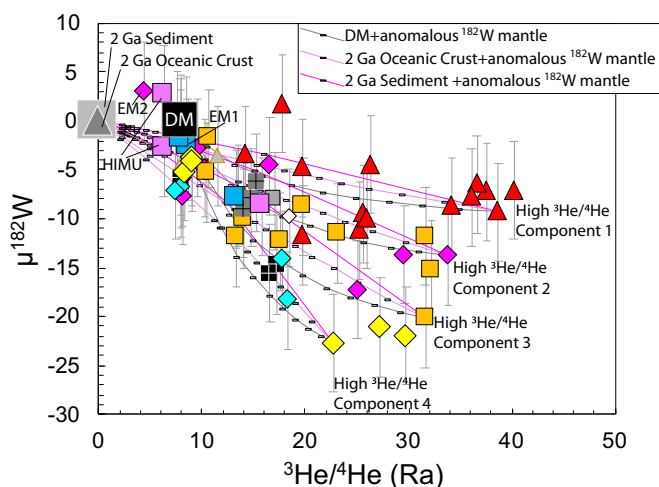
Iceland hotspot lavas require a mechanism for preserving these ancient signatures in the OIB mantle. We argue that the survival of high-$^3He/^4He$ and anomalous ^{182}W signatures in the convecting mantle will depend on whether anomalous ^{182}W and high-$^3He/^4He$ mantle domains mix with W- and ^4He-rich recycled materials, or with DM, which also has low $^3He/^4He$ and normal ^{182}W. Compared to domains with anomalous ^{182}W and high $^3He/^4He$, the mantle endmembers sampling recycled materials—EM1, EM2, and HIMU—lack anomalous $\mu^{182}W$. Subducted oceanic and continental crust have high W concentrations and will not necessarily host anomalous $\mu^{182}W$ (if derived from reservoirs that formed after the early Hadean), and they will evolve high ^4He concentrations and low $^3He/^4He$ over time (due to having higher U and Th concentrations and to loss of He during subduction) (see Datasets S5 and S6 for data sources). Thus, one hypothesis is that subducted crust can overprint high-$^3He/^4He$ and anomalous $\mu^{182}W$ signatures with low $^3He/^4He$ and normal $\mu^{182}W$, explaining why mantle domains similar to EM1, EM2, and HIMU have low $^3He/^4He$ and lack anomalous $\mu^{182}W$, while domains with high $^3He/^4He$ and anomalous $\mu^{182}W$ do not extend to extreme EM (low $^{143}Nd/^{144}Nd$) or HIMU (high $^{143}Nd/^{144}Nd$ and high $^{206}Pb/^{204}Pb$) compositions that reflect large contributions from W- and ^4He-rich recycled materials (Fig. 3 and *SI Appendix*, Fig. S5).

The addition of variable quantities of subducted materials to mantle domains with anomalous ^{182}W is a potential mechanism to explain variability in the magnitude of recently discovered ^{182}W anomalies in modern hotspot lavas. Before the discovery of ^{182}W anomalies in the present-day mantle, subduction and recycling of W-rich crust was considered as a possible mechanism to explain the complete absence of detectable core-derived ^{182}W anomalies in Earth's mantle (28, 29). However, the discovery of ^{182}W variability in the modern mantle indicates that ^{182}W heterogeneity has not been entirely overprinted with subducted crust. Thus, we explore a more nuanced version of this early model to gain new insights into the coupled ^{182}W-$^3He/^4He$ systematics of the mantle. We quantitatively examine the influence of recycled crust and DM on mantle domains that host anomalous $\mu^{182}W$ and high-$^3He/^4He$ compositions (Fig. 4).

In $\mu^{182}W$ versus $^3He/^4He$ space, the data form a negatively sloping array that is composed of subtrends formed by different hotspots (14–16), and the strength of the overall global trend is supported by a high correlation (Spearman rank coefficient $r_s = -0.67 \pm 0.07$) (Fig. 4). Assuming an average age for recycled crust of 2 Ga [an age consistent with the slope of the Northern Hemisphere Reference Line (NHRL) in Pb isotopic space (30)], we show that mixing ancient subducted oceanic and continental crust with high-$^3He/^4He$ mantle sources of OIB with anomalous $\mu^{182}W$ forms mixing trends with negatively sloping arrays that describe the coupled $\mu^{182}W$ and $^3He/^4He$ systematics of global OIB (Fig. 4).

Absolute He and W concentrations in the mantle are not well constrained, but the concentration contrast between high-$^3He/^4He$ mantle domains and subducted materials can be inferred to construct the mixing models in Fig. 4. All W and He isotopic compositions and mantle source concentrations for the model in Fig. 4 are provided in Dataset S5. Compared to the high-$^3He/^4He$ mantle, oceanic and continental crust is expected to have high concentrations of W (0.12 and 1.9 ppm, respectively) (31, 32) and ^4He, the latter due to the decay of Th and U (which are elevated in oceanic and continental crust relative to the high-$^3He/^4He$ mantle). High-$^3He/^4He$ lavas with anomalous ^{182}W from

Kroenke- and Kwaimbaita-type lavas (65); present-day mantle source compositions (23) are show in lieu of measured or age-corrected ages due to the 120-Ma eruption age. The OJP $\mu^{182}W$ data that are shown lack of anomalous signatures (41, 46).

Fig. 4. Impact of mixing subducted crust and DM on OIB mantle domains with high-^{3}He/^{4}He and anomalous μ^{182}W compositions. The mixing models demonstrate how subducted crustal materials, and DM, reduce ^{3}He/^{4}He and overprint resolvable μ^{182}W anomalies in the mantle, thereby generating the negatively sloping OIB array. Sediment (large gray box), oceanic crust (large gray triangle), and depleted mantle (DM, large black box) are each mixed with four OIB mantle sources with high ^{3}He/^{4}He and anomalous μ^{182}W. Endmember compositions are used in Dataset S5. Samoa and Hawaii have indistinguishable trends (14–16), but Samoan μ^{182}W is characterized to higher ^{3}He/^{4}He. Intervals are marked at 10% for mixtures with DM; for mixtures with sediment and oceanic crust, intervals are marked at 1% for the first 10% addition of subducted material, thereafter every 20%. Sediment (derived from continental crust) and oceanic crust, when mixed with components that have high-^{3}He/^{4}He and anomalous μ^{182}W, generate compositions similar to the extreme Samoan EM2 lava (5% subducted sediment), the extreme Pitcairn EM1 lava (3% sediment), and the extreme Mangaia HIMU lavas (25% oceanic crust) (Datasets S4 and S5). OIB data symbols are the same as in Fig. 3. OIB data and error bars (2σ) are provided in Dataset S4.

Hawaii (Loihi) provide a window into the W concentration of the high-^{3}He/^{4}He mantle, which is calculated by melt models to have W concentrations [0.011 ± 0.005 ppm W (33)] that are ~11 and 170 times lower than subducted oceanic and continental crust, respectively. The mantle sources of high-^{3}He/^{4}He lavas have He concentrations (34) that are estimated to be approximately >9 and >80 times lower than subducted oceanic and continental crust, respectively (Dataset S5). Taking these W and He concentrations as representative of the high-^{3}He/^{4}He mantle with anomalous ^{182}W, subducted crust can overwhelm the W and He budgets of high-^{3}He/^{4}He mantle domains, overprinting them with low ^{3}He/^{4}He and normal μ^{182}W, and thus generating the negatively sloping global OIB array in Fig. 4. Finally, adding DM—which likewise has low ^{3}He/^{4}He (8 Ra) and normal ^{182}W—to the high-^{3}He/^{4}He mantle also generates a negatively sloping array that follows the slope of the OIB field in μ^{182}W-^{3}He/^{4}He space [Fig. 4; DM He (34) and W (33) concentrations are provided in Dataset S5]. The takeaway message is that anomalous ^{182}W and high ^{3}He/^{4}He in plume-fed hotspots, such as Iceland, are derived from mantle domains in which these ancient signatures are not completely overprinted by recycled materials, or mixing with DM.

This model for overprinting of the high-^{3}He/^{4}He mantle by mixing with recycled oceanic and continental crust is also consistent with the generation of low ^{3}He/^{4}He and normal ^{182}W observed in OIB endmembers EM1, EM2, and HIMU (Fig. 4 and *SI Appendix, Supplementary Information Text* and Dataset S5). Other recycled materials could overprint domains with high ^{3}He/^{4}He and anomalous ^{182}W, but such materials would also need to be 1) relatively enriched in W (to effectively mask anomalous ^{182}W domains) and 2) degassed in He and enriched in Th and U

(to generate both the high ^{4}He concentrations and low ^{3}He/^{4}He that are necessary to mask high-^{3}He/^{4}He domains). Nonetheless, mixing ancient subducted continental and oceanic crust with high-^{3}He/^{4}He mantle material, as done in Fig. 4, serves to illustrate how recycled materials efficiently overprint high-^{3}He/^{4}He and anomalous ^{182}W domains in the mantle.
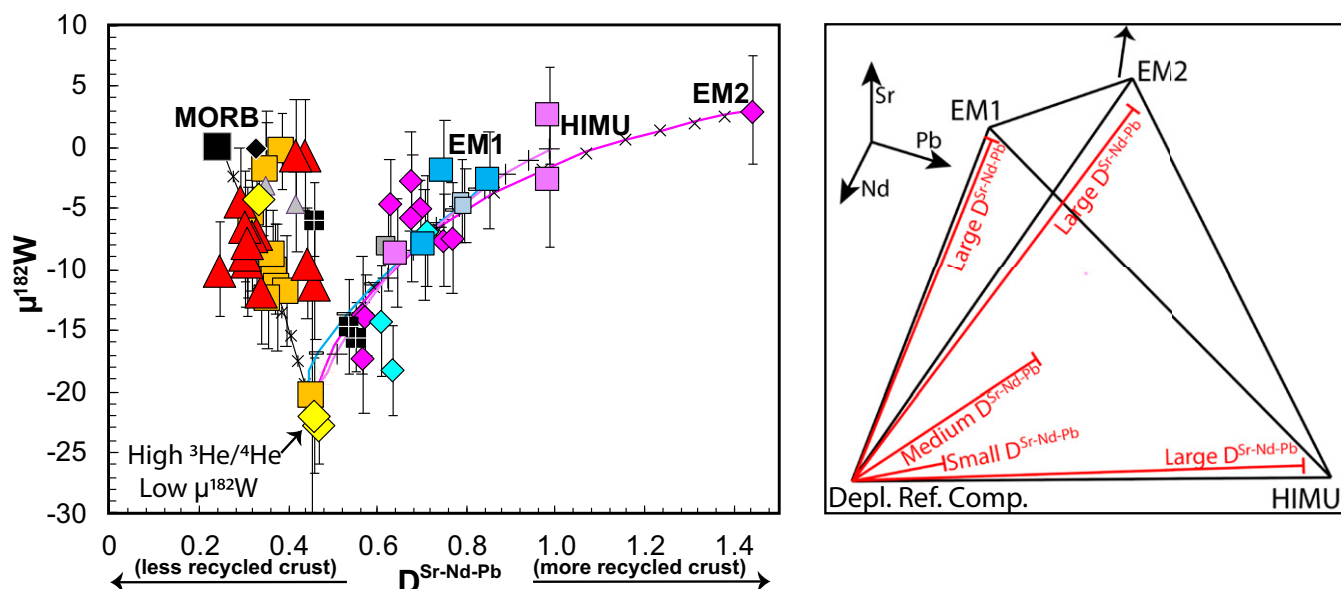
Quantifying the Relationship between ^{182}W and Crustal Recycling. It has long been assumed that addition of recycled materials to the mantle results in mantle domains with low ^{3}He/^{4}He (13, 35, 36), which is supported by the modeling exercise in Fig. 4 and the observation that mantle endmembers hosting the strongest recycling signatures in Sr-Nd-Pb isotopic space—EM1, EM2, and HIMU—have low ^{3}He/^{4}He ($\leq$8 Ra). However, the relationships between μ^{182}W and Sr-Nd-Pb isotopes and the impact of subducted materials on μ^{182}W signatures in OIB remain to be explored in detail. Armed with a dataset of Sr-Nd-Pb-W isotopes on global OIB (Dataset S4), we identify clear relationships between μ^{182}W and recycled signatures in OIB (Fig. 5).

Based on the modeling in Fig. 4, we propose that, if mixed with a high-^{3}He/^{4}He component having anomalous ^{182}W, mantle domains lacking input of recycled crust will have the most extreme negative ^{182}W anomalies, and that addition of progressively larger quantities of recycled crust will cause a reduction in the magnitude of the ^{182}W anomaly. This hypothesis is difficult to test because no single isotopic ratio is indicative of recycled materials that contribute to HIMU and recycled materials that contribute to EM1 and EM2: High ^{206}Pb/^{204}Pb can be used to identify a contribution from a HIMU component, but the ^{206}Pb/^{204}Pb ratio is less effective in identifying EM components; low ^{143}Nd/^{144}Nd and high ^{87}Sr/^{86}Sr ratios can be used to identify EM component contributions, but are less effective in identifying HIMU contributions. A single parameter is needed that indicates the magnitude of contribution from the various mantle endmembers. Therefore, we propose a "mantle endmember index" that draws on ^{87}Sr/^{86}Sr, ^{143}Nd/^{144}Nd, and ^{206}Pb/^{204}Pb to quantify the contribution of EM1–EM2–HIMU mantle endmember melt compositions to OIB lavas. This index allows evaluating how a fourth isotope system (e.g., μ^{182}W) varies in lavas as a function of the magnitude of the contribution from any of the mantle endmembers (Fig. 5). Central to this index are two assumptions: 1) Lavas sampling geochemically depleted mantle (DM)—which has low ^{206}Pb/^{204}Pb, low ^{87}Sr/^{86}Sr, and high ^{143}Nd/^{144}Nd—lack a significant component of recycled materials, and 2) an increase in the contribution of recycled material results in a shift away from the depleted mantle composition in Sr-Nd-Pb isotopic space toward HIMU and EM compositions (Fig. 5). Larger shifts correspond to greater recycled contributions.

This shift away from the geochemically depleted mantle (DM) can be measured as a distance ($D^{Sr-Nd-Pb}$) in 3D ^{87}Sr/^{86}Sr-^{143}Nd/^{144}Nd-^{206}Pb/^{204}Pb space, using the following equation:

$$D^{Sr-Nd-Pb} = \left[\left(\left(^{87}Sr/^{86}Sr_O - {}^{87}Sr/^{86}Sr_D \right)/X \right)^2 \right.$$
$$+ \left(\left(^{143}Nd/^{144}Nd_O - {}^{143}Nd/^{144}Nd_D \right)/Y \right)^2$$
$$+ \left. \left(\left(^{206}Pb/^{204}Pb_O - {}^{206}Pb/^{204}Pd_D \right)/Z \right)^2 \right]^{0.5},$$

where the subscripts O and D indicate the isotopic composition of any "OIB" sample and the geochemically "depleted" reference composition, respectively; the depleted reference composition has ^{87}Sr/^{86}Sr, ^{143}Nd/^{144}Nd, and ^{206}Pb/^{204}Pb compositions of 0.7025, 0.5132, and 17.5, respectively; X, Y, and Z represent the Sr-Nd-Pb isotopic differences between the geochemically depleted reference composition and the most extreme crustal recycling signatures in OIB considered in ^{87}Sr/^{86}Sr (0.7186 to 0.7025), ^{143}Nd/^{144}Nd (0.5132 to 0.5123), and ^{206}Pb/^{204}Pb (22.0 to 17.5) isotopic

Fig. 5. $\mu^{182}W$ as a function of $D^{Sr\text{-}Nd\text{-}Pb}$ showing that OIB sampling significant recycled crust (represented by extreme EM1, EM2, and HIMU lavas), or MORB, lack $\mu^{182}W$ anomalies. (*Left*) Samples with the lowest $D^{Sr\text{-}Nd\text{-}Pb}$ (defined in the main text) have the smallest contributions from the EM1, EM2, and HIMU mantle endmembers (and the smallest recycled crust contributions). Samples with the highest $D^{Sr\text{-}Nd\text{-}Pb}$ plot closest to EM1, EM2, and HIMU in Sr-Nd-Pb isotopic space (and host the greatest recycled crust contributions). Binary mixing lines are shown between a melt with anomalous $\mu^{182}W$ and melts of EM1 (blue line), EM2 (pink line), HIMU (purple line), and MORB melts of DM (black mixing line) (see Dataset S6 for model compositions); 10% mixing increments are shown. Symbols are the same as Fig. 3 and data (and 2σ errors) are from Dataset S4 (except for OJP data, which are indicated in Fig. 3). (*Right*) Illustration of calculation of $D^{Sr\text{-}Nd\text{-}Pb}$ values and examples of three large $D^{Sr\text{-}Nd\text{-}Pb}$ values, one medium $D^{Sr\text{-}Nd\text{-}Pb}$ value, and one small $D^{Sr\text{-}Nd\text{-}Pb}$ value; all $D^{Sr\text{-}Nd\text{-}Pb}$ values are distances in $^{87}Sr/^{86}Sr$-$^{143}Nd/^{144}Nd$-$^{206}Pb/^{204}Pb$ isotope space calculated between the depleted reference composition (Depl. Ref. Comp.) and OIB samples.

spaces, respectively. Higher values of $D^{Sr\text{-}Nd\text{-}Pb}$ for an OIB sample reflect a greater contribution from EM1, EM2, and/or HIMU (and therefore more recycled materials), while lower values indicate that lavas are more similar to the DM component and indicate a smaller contribution from these three mantle endmembers (and therefore less recycled material) (Fig. 5, *Right*). A similar parameter for measuring distance in 3D Pb isotope multispace (i.e., $D^{208/207/206Pb}$) was developed elsewhere (37) and serves as the basis for the $D^{Sr\text{-}Nd\text{-}Pb}$ parameter presented here.

Fig. 5 shows $\mu^{182}W$ in OIB as a function of $D^{Sr\text{-}Nd\text{-}Pb}$ and demonstrates that all OIB data with the most extreme negative $\mu^{182}W$ have low $D^{Sr\text{-}Nd\text{-}Pb}$ values (<0.65), consistent with the hypothesis that only lavas sampling geochemically depleted mantle domains (i.e., lacking significant recycled materials) host the most extreme negative $\mu^{182}W$ anomalies. However, many geochemically depleted lavas with low $D^{Sr\text{-}Nd\text{-}Pb}$ values lack anomalous ^{182}W, and this is accounted for by dilution of the anomalous ^{182}W by entrainment of a depleted mantle (DM) component lacking anomalous ^{182}W, which melts in the shallow mantle with the host plume, and subsequently mixes with melts of the high-$^3He/^4He$ plume component. This process is described by the binary mixing line to MORB in Fig. 5. For example, the subset of lavas from Iceland with normal $\mu^{182}W$ may result from addition of a MORB component, consistent with the mixing line between high-$^3He/^4He$ mantle melts and MORB in Fig. 5. While a depleted component has been suggested to be inherent to the Iceland plume (38, 39), it is also possible that the plume has incorporated ambient depleted upper mantle during ascent (40), consistent with our hypothesis for reduction in the magnitude of ^{182}W anomalies in the Iceland plume by mixing with DM melts.

At higher $D^{Sr\text{-}Nd\text{-}Pb}$ values, and thus increasing fractions of recycled materials, the magnitude of the $\mu^{182}W$ anomalies diminishes in lavas at hotspots that host anomalous $\mu^{182}W$. For example, at maximum contributions of recycled materials, lavas sampling endmember EM1 (Pitcairn, $D^{Sr\text{-}Nd\text{-}Pb} = 0.85$), EM2 (Samoa,

$D^{Sr\text{-}Nd\text{-}Pb} = 1.44$), and HIMU (Mangaia Island on the Macdonald hotspot track, $D^{Sr\text{-}Nd\text{-}Pb} = 0.99$) all lack $\mu^{182}W$ anomalies. Critically, the magnitude of the recycled crust signature appears to modulate the magnitude of the anomalous ^{182}W signature: OIB samples with progressively higher values of $D^{Sr\text{-}Nd\text{-}Pb}$ at the Pitcairn, Samoa, and Macdonald hotspots show diminished $\mu^{182}W$ anomalies (Fig. 5). In contrast, input of less recycled material (i.e., lower $D^{Sr\text{-}Nd\text{-}Pb}$) corresponds with increasingly negative $\mu^{182}W$ anomalies. For example, the single Pitcairn lava with a slightly negative $\mu^{182}W$ anomaly has the lowest $D^{Sr\text{-}Nd\text{-}Pb}$ in the sample suite and also the highest $^3He/^4He$ among Pitcairn lavas. This pattern is also reflected in Macdonald and Samoan hotspot samples, where lavas with the lowest $D^{Sr\text{-}Nd\text{-}Pb}$ also have the lowest $\mu^{182}W$ and the highest $^3He/^4He$ (Fig. 5). Fig. 5 further shows that the relationship between $D^{Sr\text{-}Nd\text{-}Pb}$ and $\mu^{182}W$ at these three hotspots, which sample the three canonical mantle endmembers, is consistent with binary mixing trends between the most anomalous $\mu^{182}W$ component and the recycled crust endmembers (EM1, EM2, and HIMU). The mixing trends are consistent with an increasing contribution of recycled materials being responsible for the dilution of anomalous $\mu^{182}W$ signatures (mixing model endmembers are in Dataset S6). Thus, while the exact mechanism for the Hadean origin of $\mu^{182}W$ anomalies is not known (discussed below), it is clear that crustal subduction and recycling play a central role in modulating the expression of these anomalies in OIB. Finally, we anchor the mixing models in Fig. 5 to an extreme low $\mu^{182}W$ composition (i.e., from Fernandina, Galapagos) only because this composition represents the most negative value (−22.7) in the existing OIB dataset. As the OIB $\mu^{182}W$ dataset expands in the future, we might expect highly negative $\mu^{182}W$ anomalies to be present in OIB over a range of Sr-Nd-Pb isotopic compositions and therefore over a range of $D^{Sr\text{-}Nd\text{-}Pb}$ values, just as high-$^3He/^4He$ signatures are found in lavas with heterogeneous Sr-Nd-Pb isotopic compositions and $D^{Sr\text{-}Nd\text{-}Pb}$ values (*SI Appendix*, Fig. S5). However, like high-$^3He/^4He$ lavas, we anticipate that lavas with highly negative $\mu^{182}W$ will be limited

to those with geochemically depleted isotopic compositions and low $D^{Sr-Nd-Pb}$ values, due to the masking influence of recycled materials on both high-$^3He/^4He$ and anomalous $\mu^{182}W$ signatures in the mantle.

Some hotspot localities with existing $\mu^{182}W$ data lack Sr-Nd-Pb isotopic data, and thus $D^{Sr-Nd-Pb}$ cannot be calculated. For example, Canary hotspot lavas from La Palma lack $\mu^{182}W$ anomalies (14, 41, 42) (Dataset S4) and the lavas analyzed for $\mu^{182}W$ do not have complete Sr-Nd-Pb isotopic datasets. The lack of $\mu^{182}W$ anomalies may be consistent with contribution from a HIMU component present in some La Palma lavas (43), which would be associated with high $D^{Sr-Nd-Pb}$ values that are linked to recycled crust that masks anomalous $\mu^{182}W$. If the strength of the global relationship between $\mu^{182}W$ and $^3He/^4He$ serves as a guide to which OIB host anomalous $\mu^{182}W$ (Fig. 4), then the lack of high $^3He/^4He$ at the Canaries [the highest $^3He/^4He$ value is 9.7 Ra (44)] is consistent with the absence of anomalous ^{182}W signatures.

The presence of extreme negative $\mu^{182}W$ only in global OIB with $^{143}Nd/^{144}Nd > 0.5127$ (Fig. 3) is explained by the fact that lavas with low $^{143}Nd/^{144}Nd$ values (<0.5127) may be impacted by subducted continental crust [as suggested for the low $^{143}Nd/^{144}Nd$ in EM1 (6) and EM2 (36) lavas], a mechanism that both reduces $^{143}Nd/^{144}Nd$ and masks anomalous $\mu^{182}W$. At the more geochemically depleted end of the spectrum, where additional $\mu^{182}W$ anomalies may be found in the future, there is currently a lack of OIB with existing $\mu^{182}W$ analyses. Fig. 5 calls particular attention to the lack of data among the most geochemically depleted OIB, as there is a total absence of ^{182}W-characterized lavas with $D^{Sr-Nd-Pb} < 0.25$. Given their geochemically depleted isotopic signatures (with $^{143}Nd/^{144}Nd$ up to ~0.5131) (23–25) and extreme high $^3He/^4He$ (up to 50 Ra) (23–26), the proto-Iceland plume BIWG continental flood basalts (CFB) offer an important opportunity in this regard and are discussed below. For example, the least crustally contaminated lavas among the Baffin Island suite (23) have $D^{Sr-Nd-Pb}$ ranging from 0.11 to 0.17. However, continental crust contamination represents a challenge for identifying mantle source $\mu^{182}W$ signatures in these lavas.

The Case of the BIWG High-$^3He/^4He$ CFB.
While all high-$^3He/^4He$ OIB have anomalous $\mu^{182}W$ (14–16), the high-$^3He/^4He$ West Greenland CFB lavas lack resolvable $\mu^{182}W$ anomalies in lavas with $^3He/^4He$ up to 48 Ra (15). This contrasts with results from an earlier study which reported positive $\mu^{182}W$ (up to $\mu^{182}W = +48.4$) for lavas from Baffin Island and the Ontong Java Plateau (OJP) ($\mu^{182}W = +23.9$) (45). However, $\mu^{182}W$ anomalies were not identified in analyses of OJP lavas in other studies (41, 46). Until the positive $\mu^{182}W$ for OJP and Baffin Island (15) are replicated we will not include them in further discussion in this paper. In Figs. 3 and 5 (and SI Appendix, Fig. S5) we show OJP as lacking anomalous ^{182}W (41, 46). Additionally, we rely on recent ^{182}W analyses from West Greenland (15) to constrain the composition of the proto-Iceland plume.

The absence of negative $\mu^{182}W$ anomalies in the West Greenland picrites might reflect an absence of anomalous $\mu^{182}W$ in the mantle source (15). Alternatively, it could result from shallow-level continental crust contamination that overprinted mantle-derived $\mu^{182}W$ anomalies. High $^3He/^4He$ ratios in the lavas with $\mu^{182}W$ measurements do not necessarily exclude crustal assimilation influence on the Sr-Nd-Pb-W isotopic compositions. For example, a crustally contaminated Baffin Island lava—sample BI/CS/7—has $^{87}Sr/^{86}Sr_{60} = 0.704912$ and $^{143}Nd/^{144}Nd_{60} = 0.512730$ compositions consistent with a continental crust contribution, yet the olivines preserve high $^3He/^4He$ (43.9 Ra) (24). These data suggest that crustal contamination may not impact $^3He/^4He$ in the same manner it affects the heavy radiogenic isotopic systems, possibly because $^3He/^4He$ is measured in gas trapped and preserved in olivines

formed at depth, prior to significant shallow crustal assimilation that influences the whole-rock Sr-Nd-Pb-W isotopic compositions.

Significant crustal assimilation appears unlikely in a subset of the BIWG lavas examined in several key studies (23–25). Nonetheless, the extreme enrichment of W in upper continental crust (1.9 ppm W) (31) relative to West Greenland lavas (down to 0.022 ppm) (15) suggests that small degrees of continental crust assimilation can dramatically shift $\mu^{182}W$ in the lavas, while leaving the long-lived radiogenic isotopic systems relatively unmodified, as demonstrated in SI Appendix, Supplementary Information Text. Thus, the presence of $\mu^{182}W$ anomalies in the mantle source of West Greenland lavas cannot be ruled out, since the $\mu^{182}W$ anomalies may have been obscured by small degrees of crustal assimilation. For this reason, $\mu^{182}W$ for the West Greenland picrites are not considered further here nor shown in the figures (see discussion in SI Appendix, Supplementary Information Text). The reason the West Greenland lavas are the only modern mantle-derived lavas to plot off the global OIB $\mu^{182}W$-$^3He/^4He$ array may relate to the fact that they are the only high-$^3He/^4He$ lavas with $\mu^{182}W$ analyses that erupted in a continental setting, where continental crust assimilation is a concern.

Origin of Anomalous $\mu^{182}W$ Signatures in Oceanic Hotspots.
The discovery of negative $\mu^{182}W$ values in volcanic hotspot lavas has been interpreted to reflect a geochemical influence from Earth's core (16, 17), which should have low $\mu^{182}W$ [~−220 (42)]. Similarly, ancient high $^3He/^4He$ has been suggested to reside in Earth's core (24, 47–49). Given the relationship between high $^3He/^4He$ and anomalous $\mu^{182}W$ in modern OIB, it is tempting to suggest a model where both high $^3He/^4He$ and anomalous $\mu^{182}W$ are supplied to the mantle by the core. While there are limited high-precision ^{182}W data on MORB (14), such a model could potentially explain why depleted upper mantle does not host clear ^{182}W anomalies, as the geochemically depleted upper mantle is less likely to host a component that came from or interacted with the core than lower mantle domains sampled by upwelling plumes. An advantage of this model is that it can potentially explain our observation that only geochemically depleted OIB lavas have negative $\mu^{182}W$ anomalies and high $^3He/^4He$, as any W and He emerging from the core will have a proportionally greater impact on the $^3He/^4He$ and $\mu^{182}W$ compositions of geochemically depleted mantle domains (which have low W and He concentrations) compared to mantle domains overprinted by recycled crust materials (which have high W and He concentrations and therefore are more immune to He and W isotopic signatures from the core). Furthermore, the nonprimitive Pb-isotopic composition of lavas with the most anomalous $\mu^{182}W$ compositions (Fig. 3) suggests that low $\mu^{182}W$ is not due to preservation of an ancient component in the mantle but instead is due to mixing between a depleted mantle domain and a component with low $\mu^{182}W$ and high $^3He/^4He$, a process that is consistent with a core contribution to a depleted mantle domain. However, preservation of high $^3He/^4He$ in the core is controversial, and a lower mantle origin for high $^3He/^4He$ has also been suggested (8, 10, 13). Thus, the analysis and modeling proposed here focus on the modern mantle sources and eruptive products of OIB without any assumptions regarding specific mechanisms for the origin of high $^3He/^4He$ and anomalous $\mu^{182}W$ in the mantle. Looking forward, models invoked to generate negative $\mu^{182}W$ in the silicate Earth—core addition, late accretion, or silicate Earth differentiation (16, 17, 41, 50, 51)—must also explain the link between anomalous $\mu^{182}W$ and high $^3He/^4He$ in geochemically depleted mantle sources of OIB.

Geodynamic Implications for High $^3He/^4He$ and Anomalous ^{182}W in the Mantle.
Under very restrictive conditions—in geochemically depleted mantle domains lacking recycled crust—early-Earth high-$^3He/^4He$ and anomalous $\mu^{182}W$ signatures have survived convective mixing and interaction with subducted crust to be sampled by

upwelling mantle plumes and erupted at modern hotspot volcanoes. The geodynamic process of crustal subduction and recycling plays an outsized role in the destruction of both anomalous $\mu^{182}W$ and high $^3He/^4He$ in the mantle because W and ^4He concentrations in recycled oceanic and continental crust may be higher than the respective concentrations in the high-$^3He/^4He$ mantle (by approximately one to two orders of magnitude, for oceanic and continental crust, respectively; Dataset S5). Given evidence provided by high $^3He/^4He$ and anomalous ^{182}W, the Iceland mantle plume, together with a number of other plumes globally, sample mantle domains that are relatively unmodified by crustal recycling or mixing with DM.

This geodynamic framework, which relies on the well-established mechanism of crustal subduction and recycling in the mantle, can be used to evaluate the preservation and distribution of ancient isotopic signatures in the mantle. Like anomalous ^{182}W, nucleosynthetic and short-lived radiogenic isotopic anomalies of elements enriched in Earth's crust (31, 32) relative to the mantle (52) [e.g., ^{142}Nd (18), or even nucleosynthetic ^{92}Mo if heterogeneities are detected in the modern mantle (53)] may be expected to survive primarily in geochemically depleted mantle domains least influenced by recycling. Similarly, nucleosynthetic isotopic signatures for ^{100}Ru (54), if found in the modern mantle (53), would be expected to be less impacted by crustal subduction and recycling than W, because Ru is concentrated in the mantle (52) relative to the crust (31). This would also be the case for elements that are concentrated in the crust or atmosphere relative to the mantle but are not as efficiently subducted into the mantle as W [e.g., ^{129}Xe (55)]. Finally, preservation of ancient high-$^3He/^4He$ and anomalous $\mu^{182}W$ signatures in the mantle requires isolation of the high-$^3He/^4He$ mantle from subducted crust (56). Due to having higher viscosity, which slows convective motions, the deep lower mantle is an ideal location to preserve ancient domains. The ultra-low velocity zones (ULVZs) may host anomalous $\mu^{182}W$ (16), and the large low shear wave velocity provinces (LLSVPs) are suggested to host high $^3He/^4He$ (57). If the LLSVPs (58–60) or ULVZs (61) are denser than ambient mantle, and thus more difficult to entrain, the observation that high $^3He/^4He$ is entrained only by the hottest, most buoyant plumes is more easily explained (62) (SI Appendix, Fig. S6). Expanded datasets covering a greater geographic range of hotspots with lower buoyancy fluxes will be important for extending these geophysical relationships to $\mu^{182}W$.

Materials and Methods

We present whole-rock Sr-Nd-Hf-Pb-W isotopic and major and trace element data, $^3He/^4He$ data obtained on olivines and clinopyroxenes (by crushing and fusion), and olivine major element data for a suite of 18 mid-Miocene lavas from northwest Iceland (Vestfirðir) (Datasets S1–S3 and S7). Vestfirðir sample locations, constraints on sample ages, descriptions, and age corrections for Sr-Nd-Hf-Pb isotopic compositions are also provided (Datasets S1, S8, and S9). Additionally, we present Sr-Nd-Hf-Pb isotopic data (as well as W isotopic data for ERZ sample A24) for five samples from the SIVZ (20.7 to 25.7 Ra), four samples from the ERZ (20.6 to 25.9 Ra), and one NRZ sample from Vaðalda (33.6 Ra) (Datasets S1 and S3). Protocols for wet chemistry and radiogenic isotopic analyses (Sr-Nd-Hf-Pb) follow standard techniques and were carried out at four different institutions by TIMS (thermal ionization mass spectrometry) or MC-ICP-MS (multicollector inductively coupled plasma mass spectrometry) following methods detailed in SI Appendix, Materials and Methods: ENS Lyon (Ecole Normale Supérieure de Lyon: Hf and Pb isotopes by MC-ICP-MS), UCSB (University of California, Santa Barbara: Sr and Nd isotopes by TIMS), UNC (University of North Carolina: Sr and Nd isotopes by TIMS), and USC (University of South Carolina: Sr, Nd, Hf, and Pb isotopes by MC-ICP-MS). Methods for analysis of W isotopes at the University of Vienna are provided elsewhere (SI Appendix, Materials and Methods). Measurements of He isotopes, carried out at WHOI (Woods Hole Oceanographic Institution), follow standard protocols (SI Appendix, Materials and Methods). Whole-rock major and trace element analyses were carried out at the GeoAnalytical Lab at Washington State University following standard protocols (SI Appendix, Materials and Methods). All data and protocols associated with this work are provided in SI Appendix.

Data Availability. All study data are included in the paper, SI Appendix, and Datasets S1–S9.

1. A. Zindler, S. R. Hart, Chemical geodynamics. *Annu. Rev. Earth Planet. Sci.* **14**, 493–571 (1986).
2. A. W. Hofmann, W. M. White, Mantle plumes from ancient oceanic crust. *Earth Planet. Sci. Lett.* **57**, 421–436 (1982).
3. W.M. White, A.W. Hofmann, Sr and Nd isotope geochemistry of oceanic basalts and mantle evolution. *Nature* **296**, 821–825 (1982).
4. S. Pilet, M. B. Baker, E. M. Stolper, Metasomatized lithosphere and the origin of alkaline lavas. *Science* **320**, 916–919 (2008).
5. Y. Weiss, C. Class, S. L. Goldstein, T. Hanyu, Key new pieces of the HIMU puzzle from olivines and diamond inclusions. *Nature* **537**, 666–670 (2016).
6. J. Eisele, M. Sharma, S.J.G. Galer, J. Blichert-Toft, C.W. Devey, A.W. Hofmann, The role of sediment recycling in EM-1 inferred from Os, Pb, Hf, Nd, Sr isotope and trace element systematics of the Pitcairn hotspot. *Earth Planet. Sci. Lett.* **196**, 197–212 (2002).
7. P. R. Castillo, C. MacIsaac, S. Perry, J. Veizer, Marine carbonates in the mantle source of oceanic basalts: Pb isotopic constraints. *Sci. Rep.* **8**, 14932 (2018).
8. S. R. Hart, E. H. Hauri, L. A. Oschmann, J. A. Whitehead, Mantle plumes and entrainment: Isotopic evidence. *Science* **256**, 517–520 (1992).
9. D. W. Graham, "Noble gas isotope geochemistry of midocean ridge and ocean island basalts; characterization of mantle source reservoirs" in *Noble Gases in Geochemistry and Cosmochemistry*, D. Porcelli, C. J. Ballentine, R. Wieler, (Reviews in Mineralogy and Geochemistry, De Gruyter, 2002), vol. 47, pp. 247–318.
10. C. Class, S. L. Goldstein, Evolution of helium isotopes in the Earth's mantle. *Nature* **436**, 1107–1112 (2005).
11. K. A. Farley, J. H. Natland, H. Craig, Binary mixing of enriched and undegassed (primitive?) mantle components (He, Sr, Nd, Pb) in Samoan lavas. *Earth Planet. Sci. Lett.* **111**, 183–199 (1992).
12. B. B. Hanan, D. W. Graham, Lead and helium isotope evidence from oceanic basalts for a common deep source of mantle plumes. *Science* **272**, 991–995 (1996).
13. M. D. Kurz, W. J. Jenkins, S. R. Hart, Helium isotopic systematics of oceanic islands and mantle heterogeneity. *Nature* **297**, 43–47 (1982).
14. A. Mundl et al., Tungsten-182 heterogeneity in modern ocean island basalts. *Science* **356**, 66–69 (2017).
15. A. Mundl-Petermeier et al., Temporal evolution of primordial tungsten-182 and $^3He/^4He$ signatures in the Iceland mantle plume. *Chem. Geol.* **525**, 245–259 (2019).
16. A. Mundl-Petermeier et al., Anomalous ^{182}W in high $^3He/^4He$ ocean island basalts: Fingerprints of Earth's core? *Geochim. Cosmochim. Acta* **271**, 194–211 (2020).
17. H. Rizo et al., ^{182}W evidence for core-mantle interaction in the source of mantle plumes. *Geochem. Perspect. Lett.* **11**, 6–11 (2019).
18. B. J. Peters, R. W. Carlson, J. M. D. Day, M. F. Horan, Hadean silicate differentiation preserved by anomalous $^{142}Nd/^{144}Nd$ ratios in the Réunion hotspot source. *Nature* **555**, 89–93 (2018).
19. S. Mukhopadhyay, Early differentiation and volatile accretion recorded in deep-mantle neon and xenon. *Nature* **486**, 101–104 (2012).
20. S. Harðardóttir, S. A. Halldórsson, D. E. Hilton, Spatial distribution of helium isotopes in Icelandic geothermal fluids and volcanic materials with implications for location, upwelling and evolution of the Icelandic mantle plume. *Chem. Geol.* **480**, 12–27 (2018).
21. D. R. Hilton, K. Grönvold, C. G. Macpherson, P. R. Castillo, Extreme $^3He/^4He$ ratios in northwest Iceland: Constraining the common component in mantle plumes. *Earth Planet. Sci. Lett.* **173**, 53–60 (1999).
22. C. G. Macpherson, D. R. Hilton, J. M. D. Day, D. Lowry, K. Grönvold, High-$^3He/^4He$, depleted mantle and low-$\delta^{18}O$, recycled oceanic lithosphere in the source of central Iceland magmatism. *Earth Planet. Sci. Lett.* **233**, 411–427 (2005).
23. L. N. Willhite et al., Hot and heterogenous high-$^3He/^4He$ components: New constraints from proto-Iceland plume lavas from Baffin Island. *Geochem. Geophys. Geosyst.* **20**, 5939–5967 (2019).
24. N. A. Starkey et al., Helium isotopes in early Iceland plume picrites: Constraints on the composition of high $^3He/^4He$ mantle. *Earth Planet. Sci. Lett.* **277**, 91–100 (2009).

25. D. W. Graham *et al*., Helium isotope composition of the early Iceland mantle plume inferred from the Tertiary picrites of West Greenland. *Earth Planet. Sci. Lett.* **160**, 241–255 (1998).

26. F. M. Stuart, S. Lass-Evans, J. G. Fitton, R. M. Ellam, High ^{3}He/^{4}He ratios in picritic basalts from Baffin Island and the role of a mixed reservoir in mantle plumes. *Nature* **424**, 57–59 (2003).

27. J. G. Konter *et al*., One hundred million years of mantle geochemical history suggest the retiring of mantle plumes is premature. *Earth Planet. Sci. Lett.* **275**, 285–295 (2008).

28. A. D. Brandon, R. J. Walker, The debate over core–mantle interaction. *Earth Planet. Sci. Lett.* **232**, 211–225 (2005).

29. O. Nebel, P. Z. Vroon, D. F. Wiggers de Vries, F. E. Jenner, J. A. Mavrogenes, Tungsten isotopes as tracers of core–Mantle interactions: The influence of subducted sediments. *Geochim. Cosmochim. Acta* **74**, 751–762 (2010).

30. S. R. Hart, A large-scale isotope anomaly in the Southern Hemisphere mantle. *Nature* **309**, 753–757 (1984).

31. R. L. Rudnick, S. Gao, "Composition of the continental crust" in *Treatise on Geochemistry*, H. D. Holland, K. K. Turekian, Eds. (Elsevier, 2003), pp. 1–64.

32. A. Gale, C. A. Dalton, C. H. Langmuir, Y. Su, The mean composition of ocean ridge basalts. *Geochem. Geophys. Geosyst.* **14**, 489–518 (2013).

33. T. I. Ireland, R. Arevalo Jr, R. J. Walker, W. F. McDonough, Tungsten in Hawaiian picrites: A compositional model for the sources of Hawaiian lavas. *Geochim. Cosmochim. Acta* **73**, 4517–4530 (2009).

34. D. Porcelli, C. J. Ballentine, Models for the distribution of terrestrial noble gases and evolution of the atmosphere. *Rev. Mineral. Geochem.* **46**, 411–480 (2002).

35. T. Hanyu, I. Kaneoka, The uniform and low ^{3}He/^{4}He ratios of HIMU basalts as evidence for their origin as recycled materials. *Nature* **390**, 273–276 (1997).

36. M. G. Jackson *et al*., The return of subducted continental crust in Samoan lavas. *Nature* **448**, 684–687 (2007).

37. M. G. Jackson *et al*., Helium and lead isotopes reveal the geochemical geometry of the Samoan plume. *Nature* **514**, 355–358 (2014).

38. J. G. Fitton, A. D. Saunders, P. D. Kempton, B. S. Hardarson, Does depleted mantle form an intrinsic part of the Iceland plume? *Geochem. Geophys. Geosyst.*, 10.1029/2002GC000424 (2003).

39. A. C. Kerr, A. D. Saunders, J. Tarney, N. H. Berry, V. L. Hards, Depleted mantle-plume geochemical signature: No paradox for plume theories. *Geology* **23**, 843–846 (1995).

40. B. B. Hanan, J. Blichert-Toft, R. Kingsley, J.-G. Schilling, Depleted Iceland mantle plume geochemical signature: Artifact of multicomponent mixing? *Geochem. Geophys. Geosyst.*, 10.1029/1999GC000009 (2000).

41. M. Willbold, T. Elliott, S. Moorbath, The tungsten isotopic composition of the Earth's mantle before the terminal bombardment. *Nature* **477**, 195–198 (2011).

42. M. Touboul, I. S. Puchtel, R. J. Walker, ^{182}W evidence for long-term preservation of early mantle differentiation products. *Science* **335**, 1065–1069 (2012).

43. A. Klügel, K. Galipp, K. Hoernle, F. Hauff, S. Groom, Geochemical and volcanological evolution of La Palma, Canary islands. *J. Pet.* **58**, 1227–1248 (2017).

44. J. M. D. Day, D. R. Hilton, Origin of ^{3}He/^{4}He ratios in HIMU-type basalts constrained from Canary Island lavas. *Earth Planet. Sci. Lett.* **305**, 226–234 (2011).

45. H. Rizo *et al*., Preservation of Earth-forming events in the tungsten isotopic composition of modern flood basalts. *Science* **352**, 809–812 (2016).

46. T. S. Kruijer, T. Kleine, No ^{182}W excess in the Ontong Java Plateau source. *Chem. Geol.* **485**, 24–31 (2018).

47. C. G. Macpherson, D. R. Hilton, J. M. Sinton, R. J. Poreda, H. Craig, High ^{3}He/^{4}He ratios in the Manus backarc basin: Implications for mantle mixing and the origin of plumes in the western Pacific Ocean. *Geology* **26**, 1007–1010 (1998).

48. D. Porcelli, A. N. Halliday, The core as a possible source of mantle helium. *Earth Planet. Sci. Lett.* **192**, 45–56 (2001).

49. M. A. Bouhifd, A. P. Jephcoat, V. S. Heber, S. P. Kelley, Helium in Earth's early core. *Nat. Geosci.* **6**, 982–986 (2013).

50. I. S. Puchtel, J. Blichert-Toft, M. Touboul, M. F. Horan, R. J. Walker, The coupled ^{182}W-^{142}Nd record of early terrestrial mantle differentiation. *Geochem. Geophys. Geosyst.* **17**, 2168–2193 (2016).

51. M. Willbold, S. J. Mojzsis, H. W. Chen, T. Elliott, Tungsten isotope composition of the Acasta Gneiss Complex. *Earth Planet. Sci. Lett.* **419**, 168–177 (2015).

52. W. F. McDonough, "Compositional model for the Earth's core" in *Treatise on Geochemistry*, H. D. Holland, K. K. Turekian, Eds. (Elsevier, ed. 2, 2014), pp. 559–577.

53. R. J. Walker *et al*., In search of late-stage planetary building blocks. *Chem. Geol.* **411**, 125–142 (2015).

54. M. Fischer-Gödde *et al*., Ruthenium isotope vestige of Earth's pre-late-veneer mantle preserved in Archaean rocks. *Nature* **579**, 240–244 (2020).

55. R. Parai, S. Mukhopadhyay, Xenon isotopic constraints on the history of volatile recycling into the mantle. *Nature* **560**, 223–227 (2018).

56. W. M. White, Isotopes, DUPAL, LLSVPs, and Anekantavada. *Chem. Geol.* **419**, 10–28 (2015).

57. C. D. Williams, S. Mukhopadhyay, M. L. Rudolph, B. Romanowicz, Primitive helium is sourced from seismically slow regions in the lowermost mantle. *Geochem. Geophys. Geosyst.* **20**, 4130–4145 (2019).

58. B. H. Heyn, C. P. Conrad, R. G. Trønnes, Stabilizing effect of compositional viscosity contrasts on thermochemical piles. *Geophys. Res. Lett.* **45**, 7523–7532 (2018).

59. H. C. P. Lau *et al*., Tidal tomography constrains Earth's deep-mantle buoyancy. *Nature* **551**, 321–326 (2017).

60. J. Trampert, F. Deschamps, J. Resovsky, D. Yuen, Probabilistic tomography maps chemical heterogeneities throughout the lower mantle. *Science* **306**, 853–856 (2004).

61. K. Idehara, Structural heterogeneity of an ultra-low-velocity zone beneath the Philippine Islands: Implications for core-mantle chemical interactions induced by massive partial melting at the bottom of the mantle. *Phys. Earth Planet. Inter.* **184**, 80–90 (2011).

62. M. G. Jackson, J. G. Konter, T. W. Becker, Primordial helium entrained by the hottest mantle plumes. *Nature* **542**, 340–343 (2017).

63. R. K. Workman, S. R. Hart, Major and trace element composition of the depleted MORB mantle (DMM). *Earth Planet. Sci. Lett.* **231**, 53–72 (2005).

64. A. Bouvier, J. D. Vervoort, P. J. Patchett, The Lu–Hf and Sm–Nd isotopic composition of CHUR: Constraints from unequilibrated chondrites and implications for the bulk composition of terrestrial planets. *Earth Planet. Sci. Lett.* **273**, 48–57 (2008).

65. M. L. G. Tejada *et al*., "Pin-pricking the elephant: Evidence on the origin of the Ontong Java Plateau from the Pb-Sr-Nd isotopic characteristics of ODP Leg 192 basalts," in *Origin and Evolution of the Ontong Java Plateau*, J. G. Fitton, J. J. Mahoney, P. J. Wallace, A. D. Saunders, Eds. (Special Publication 229, Geological Society of London, 2004), pp. 133–150.

EARTH, ATMOSPHERIC, AND PLANETARY SCIENCES